

# THE INFLUENCE OF MELT PRACTICE ON FINAL FATIGUE PROPERTIES OF SUPERELASTIC NITI WIRES

Matt Reinoehl\*, David Bradley\*, Ray Bouthot\*, James Proft\*\*

\*Fort Wayne Metals Research Products Corp., \*\*Metallurgical Solutions

## ABSTRACT

The impact of original melt practice and strain amplitude on Ni 56wt%-Ti wire was investigated using rotary beam fatigue testing. The fatigue tests were conducted in the superelastic condition above the Active Austenite Finish Temperature (Active  $A_f$ ). Under equivalent reduction practices to 0.267 mm, the materials demonstrated equivalent fatigue behavior, regardless of statistically detectable differences in carbon level, inclusion content, unloading plateau strength, and Active  $A_f$ .

## INTRODUCTION

Initially carbon content is noted as the primary difference between two supply sources of NiTi materials. It is important to understand whether carbon levels or other subsequently observed material characteristics effect the fatigue characteristics of finished product that will be manufactured from the differing supplies. Components made of NiTi materials are typically designed to take advantage of the superelastic and shape memory characteristics that expose a majority of these components to cyclic fatigue.

The basis of our comparison was the fatigue characteristics of NiTi wire by utilizing a rotary beam fatigue test. The impact of supply source in relation to fatigue life at various strain amplitudes was studied. Differential Scanning Calorimetry (DSC), Active  $A_f$  testing and stress/strain data was compared from finished samples to verify the equivalency of the processed materials.

## EXPERIMENTAL PROCEDURE

### Material Comparison

Redraw material obtained from Supplier A will be noted as Supply A and was characterized by a 0.0033 wt.% carbon per the melt source certification. Redraw material obtained from Supplier B, will be noted as Supply B and was characterized by a 0.0365 wt.% carbon per the melt source certification. DSC measured the Austenite Start Transformation temperatures ( $A_s$ ) of the specimens in the as received diameters, in the fully annealed condition.  $A_s$  temperatures of -29.3 °C and -29.4°C were measured for Supply A and Supply B respectively. Inclusion rating analysis was performed on samples from both supplies. Results of these tests for 10 samples are summarized in the Table below.

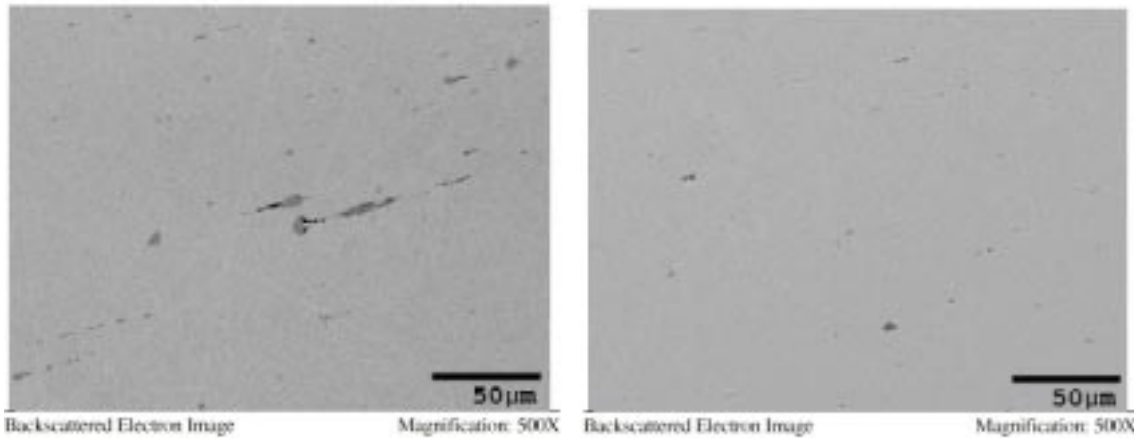
Table 1: Results of inclusion analysis

Inclusion Characteristics	Supply A (Figure 1)	Supply B (Figure 2)
Total Inclusions	17180	33700
> 2um inclusions	1205	359
Largest inclusion size	10µm	5µm
Stringer length (average)	3451µm	384µm

Examples of the general morphology of inclusions for both supplies are demonstrated in the following figures:

Figure 1: Inclusions found in Supply A

Figure 2: Inclusions found in Supply B



EDS analysis of the inclusions detected significantly more titanium and less nickel than the typical metal, possibly indicating titanium nitride. More nickel was detected for the inclusions in Supply A than Supply B.

The materials were cold drawn to a diameter of 0.267mm and thermally treated to 500°C to achieve superelastic conditions at room temperature. The wires were cut to the required length for the various strain levels used in the rotary beam fatigue testing, for tensile testing, and for the Active  $A_f$  testing.

The following table summarizes the average data collected from both supplies:

Table 2: Mechanical Properties

Material Characteristic (Mean)	Supply A	Supply B
Ultimate Tensile	1475.1 N/mm <sup>2</sup>	1498.9 N/mm <sup>2</sup>
% Elongation to Failure	14.2%	14.2%
Loading Plateau Strength	628.9 N/mm <sup>2</sup>	618.9 N/mm <sup>2</sup>
Unloading Plateau Strength	265.7 N/mm <sup>2</sup>	243.0 N/mm <sup>2</sup>
Active $A_f$	9.3 °C	13.6 °C

Unloading plateau strength and Active  $A_f$  data demonstrated, with at least a 95% level of confidence, unequal average data between supplies. All other material characteristics demonstrated, with a least a 95% level of confidence, statistical equivalency between supplies.

### Rotary Beam Fatigue Test Protocol

Fatigue data was collected utilizing rotary beam fatigue testing in an reverse osmosis water bath environment at an ambient temperature of 22°C ( $\pm$  4°C).

The testing instrument consists of a motor-driven chuck and an adjustable bushing support that allows variable positioning of the free end of the test specimen so that the axis of the chuck and axis of rotation of the loose wire end in the bushing are exactly parallel. The testing apparatus operates at a cycle speed of 3600 revolution per minute (rpm). It is synchronous to an electronic clock, which gives the apparatus an accuracy of 36 revolutions.

Two (2) support guides hold the specimen in a horizontal plane, near but not in the region of maximum strain. The guides prevent vibration, and are mounted on Alnico magnets so that they may be positioned anywhere on the steel apron of the instrument. (Figure 3.)

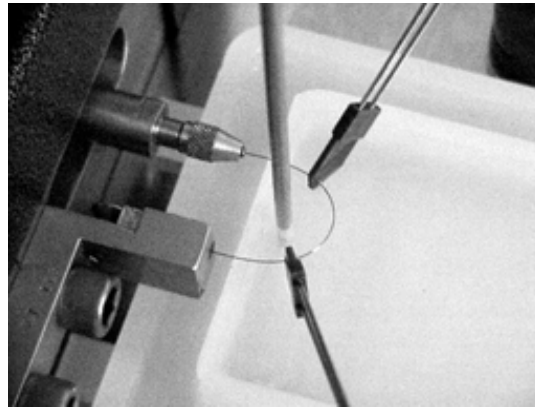


Figure 3: Rotary Beam Fatigue Tester Set Up.

The six strain values were calculated by using a starting bend radius of 6.35mm and incrementally increasing each center distance by 3.175mm. Strain values ranged from 2.1% to 0.6%.

A test is made by:

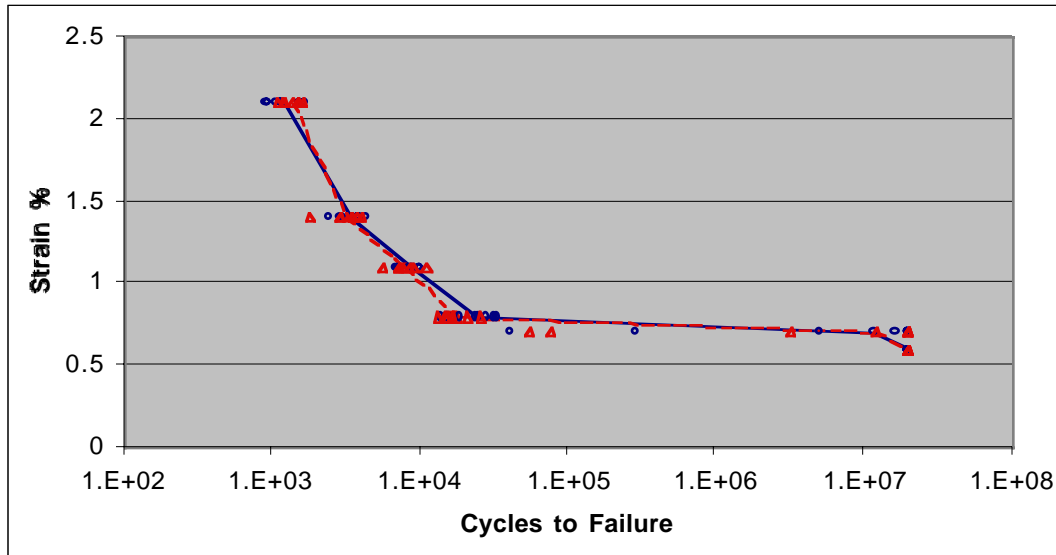
1. Calculating the specimen length “L” by using the known center distance “C” and wire diameter “d”.
2. Cutting the proper sample length, clamping it in the drive chuck and inserting the other end in the free bushing.
3. Positioning the two sample support guides outside the apex of the arc.
4. Submerging the sample in the reverse osmosis water. The temperature of the reverse osmosis water was monitored at each test specimen for verification purposes.
5. Running the test specimen until fracture or until the run out criteria of 20,000,000 cycles has been completed. The instrument is so arranged electrically that the specimen itself is grounded and a small electrical circuit is activated and the test is automatically terminated at fracture.

Fracture specimens were then submerged in isopropyl alcohol, dried, measured for length and inserted into sample bottles, with the fracture ends isolated from damage.

## RESULTS AND DISCUSSION

Fatigue tests were conducted on 0.267mm samples from both supplies. Two strain amplitude ( $\epsilon_a$ ) vs. fatigue life ( $N_f$ ) curves are shown in Figure 4 with the average data for six different strain levels plotted. Comparison of average data points between supplies at each strain level indicated equivalent means between supplies with at least a 95% level of confidence. The fatigue behavior of both samples demonstrated expected high cycle behavior at low strain levels and strain dependent, low cycle behavior at higher strain levels.<sup>2</sup> Of interest was a significant increase in the standard deviation of data at 0.7% strain level for both supplies. This increase in standard deviation was found to be statistically equivalent between both supplies with at least a 95% level of confidence.

Figure 4:  $\epsilon$  vs  $N$  Diagram Supply A is shown as circles and solid line. Supply B is shown as triangles and dashed line.



Samples tested at the 0.7% strain level from both supplies varied from 40,068 cycles to failure to 20,000,000 cycles, at which point testing was stopped. This demonstrated an average fatigue life of 10,496,000. Justification for this behavior could be found in concluding that the 0.7% strain rate corresponded directly to the critical stress needed for a martensitic transformation in both samples. Subsequent martensitic transformation may or may not be activated at this strain level at fatigue nucleation sites. These fatigue conditions may be extremely sensitive to subtle differences in the available fatigue nucleation sites within a particular sample. The fatigue nucleation sites could be inclusions or grain boundaries of adequate stress concentration.<sup>3</sup>

Fracture nucleation sites from both supplies can be noted in the SEM photos represented in Figure 5 and Figure 6. The selected photos are typical of material that experienced early fractures at a strain level of 0.7%. EDS analysis reported that the primary nucleation sites consist of a titanium rich particle with minor amounts of sodium and nickel and trace amounts of aluminum and chlorine which is sized at approximately 10 $\mu$ m. The fracture in both cases initiates from the inclusion and the balance of the cross section is covered with ductile dimples characteristic of tensile overload.

Figure 5: Inclusion/Initiation point of failure at 0.7% Strain for Supply A.

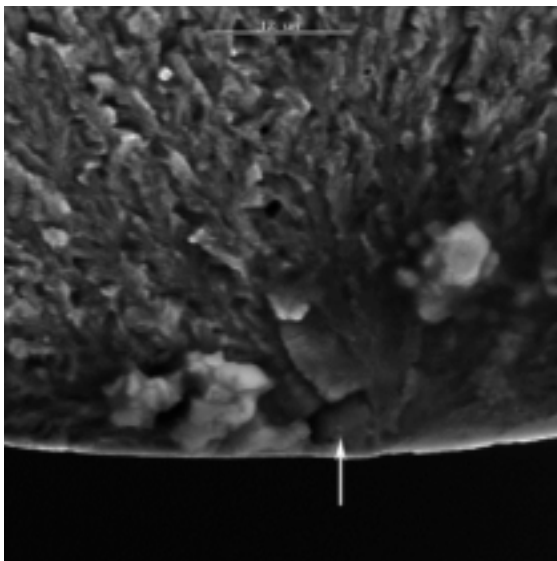
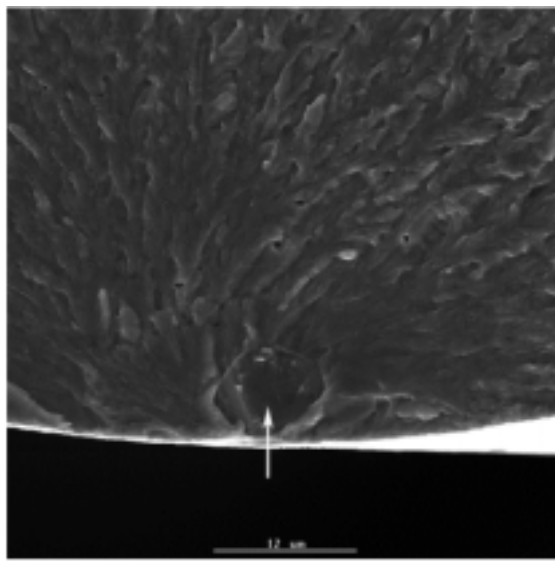


Figure 6: Inclusion/Initiation point of failure at 0.7% Strain for Supply B.



## CONCLUSIONS

The fatigue life of binary NiTi with 56 wt.% nominal Ni wire originating from two different melt sources was investigated. Under equivalent reduction practices and annealing practices to 0.267 mm, the materials demonstrated equivalent fatigue behavior, above the Af temperature, regardless of statistically detectable differences in carbon level, inclusion content, lower plateau strength at finish size, and Af temperature at finish size. Both materials did exhibit an equivalent large standard deviation in fatigue behavior at a 0.7% strain level indicating a transitional onset of a martensitic transformation within both supplies microstructures. A recommendation for further study would be smaller diameter materials. Such a study could provide conditions for investigating a possible threshold at which inclusion morphology would impact fatigue performance.

## REFERENCES

1. Operating manual, Valley Instrument Company, Rotary Beam U-Bend Wire Spin Fatigue Tester Model 10-040.
2. Y.S. Kim, S. Miyazaki, "Fatigue Properties of Ti-50.9at%Ni Shape Memory Wires." Proceedings: SMST-97, 1997, p. 473-477.
3. Miyasaki, S., "Thermal and Stress Cycling Effects and Fatigue Properties of Ni-Ti Alloys." Engineering Aspects of Shape Memory Alloys, Butterworth-Heinemann Ltd., 1990. p.394-411